

## LINEARIZAÇÃO DA UMIDADE RELATIVA SOBRE O OCEANO PACÍFICO NA LINHA EQUATORIAL

## LINEARIZATION OF RELATIVE HUMIDITY OVER THE PACIFIC OCEAN ON THE EQUATORIAL LINE

DÍEZ, César Manuel<sup>1\*</sup>; SOLANO, Carlos Javier<sup>1</sup> Universidad Nacional de ingeniería. Facultad de Ciencias, Unidad de Postgrado, Lima – Peru

\* Correspondence author

e-mail: cdiezch@uni.pe

Received 19 August 2019; received in revised form 28 October 2019; accepted 30 October 2019

## RESUMO

O sistema atmosférico é regido pela interação de muitos parâmetros meteorológicos causando dependência entre eles, ou seja, umidade e temperatura, ambos adequados diante de qualquer anomalia, como tempestades, furacões, eventos El Niño Oscilação Sul (ENSO). Portanto, entender perturbações da variação de umidade ao longo do tempo pode fornecer um indicador de qualquer fenômeno oceanográfico. Os dados anuais de umidade relativa ao redor da linha Equatorial do Oceano Pacífico foram processados e analisados para compreender a evolução temporal de cada conjunto de dados, apreciar anomalias, tendências, histogramas e propor uma maneira de prever episódios anômalos como eventos ENSO, observando anormalidade dos coeficientes de correlação de lag entre cada par de boias. Os conjuntos de dados foram retirados do projeto Rede Transoceânica de Oceano / Triângulo de Atmosfera Tropical (TAO / TRITON), matriz dirigida pelo *Pacific Environmental Laboratory* (PMEL) da Administração Nacional Oceânica e Atmosférica (NOAA) e pela Agência Japonesa de Ciências da Terra-Marinha e Tecnologia (JAMSTEC). Todos os conjuntos de dados foram processados e o código foi elaborado pelo autor ou adaptado da Mathworks Inc. Mesmo ocorrências de umidade relativa no lado leste do Oceano Pacífico parecem oscilar harmonicamente, enquanto ocorrências no lado oeste não, devido ao tamanho de suas amplitudes de oscilações. Esse fato pode ser observado nos histogramas que mostraram formas de pico no lado leste do oceano e gaussianos no oeste; As funções de correlação de defasagem mostraram que nenhum par de boias sincroniza flutuações, mas as boias ocidentais são afetadas diante dos eventos do ENSO, especialmente entre 1997-98. Definitivamente, as correlações de atraso nas boias ocidentais são determinantes para detectar eventos ENSO.

**Palavras-chave:** *Correlação Lag, eventos ENSO, Função de Distribuição Discreta, Umidade Relativa, Processo de Dados.*

## ABSTRACT

The atmosphere system is ruled by the interaction of many meteorological parameters, causing a dependency between them, i.e., moisture and temperature, both suitable in front of any anomaly, such as storms, hurricanes, El Niño-Southern Oscillation (ENSO) events. So, understanding perturbations of the variation of moistness along the time may provide an indicator of any oceanographic phenomenon. Annual relative humidity data around the Equatorial line of the Pacific Ocean were processed and analyzed to comprehend the time evolution of each dataset, appreciate anomalies, trends, histograms, and propose a way to predict anomalous episodes such ENSO events, observing abnormality of lag correlation coefficients between every pair of buoys. Datasets were taken from the Tropical Atmosphere Ocean / Triangle Trans-Ocean Network (TAO/TRITON) project, array directed by Pacific Environmental Laboratory (PMEL) of the National Oceanic and Atmospheric Administration (NOAA), and the Japan Agency for Marine-Earth Science and Technology (JAMSTEC). All the datasets were processed, and the code was elaborated by the author or adapted from Mathworks Inc. Even occurrences of relative humidity in the east side of the Pacific Ocean seem to oscillate harmonically, while occurrences in the west side, do not, because of the size of their amplitudes of oscillations. This fact can be seen in the histograms that show Peak shapes in the east side of the ocean, and Gaussians in the west; lag correlation functions show that no one pair of buoys synchronize fluctuations, but western buoys are affected in front of ENSO events, especially between 1997-98. Definitely, lag correlations in western buoys are determined to detect ENSO events.

**Keywords:** *Lag correlation, ENSO events, Discrete Distribution Function, Relative Humidity, Data process.*

## 1. INTRODUCTION

The atmosphere is thermodynamic permeable container plenty of gases (air), with a shape of a sphere that envelops the Earth. Continuously, these gases are going from one place to another inside this container in any direction, forming hurricanes (Uccellini and Ten Hoeve, 2019), storms (Gomez, Carter, Trustrum, Page, and Orpin, 2013), or just moving as winds (Xu et al., 2019), absorbing or detaching vapor water from their environment (Behar, Sbarbaro, Marzo, and Moran, 2019), reason why this gas, might be structured into two kinds, wet and dry, which percentage depends on many meteorological parameters (Xu, Huang, Zhang, and Li, 2018). Vapor water (Lawrence, 2016) may be formed upon sea surface because of the refracted radiations (Maksin et al., 2018), evaporations of surface waters (Kolehmainen et al., 2017), turbulence (Cuxart, and Jiménez, 2006), or because of rain (Chakraborty, Talukdar, Saha, Jana, and Maitra, 2017), among others.

Nevertheless, vapor water is affected by solar radiation (Riavo et al., 2016), dust concentration (Csavina, Field, Félix, Corral-Avitia, Sáez, and Betterton, 2014), biological processes (Quagliarini, Gianangeli, D'Orazio, Gregorini, Osimani, Aquilanti, and Clementi, 2019), temperature (Njau, 1994).

All these happenings criticize the amount of moisture presented in the air, affecting not only the natural environment, such as ships or embarkations travelling around, that may contain subtle merchandise such foods, electronic equipment, or the equipment of the embarkations themselves (Ju, Zhao, Mujumdar, Fang, Gao, Zheng, and Xiao, 2018, and Testaa, Maranob, Ambrogib, Boracchib, Casulac, Biganzolib, and Moroni, 2017); their crew (Buonocore, De Vecchi, Scalco, and Lamberts, 2018); or the skin (Klaassen, Schipper, and Masen, 2016).

But winds may displace these vapors to adjoining areas affecting contiguous populations (Lima, Ha Ahna, and Hwan Jeongb, 2018), animals (Xiong, Meng, Gao, Tang, Zhang, 2017), climates (Sahin & Cigizoglu, 2012), systems (Gehan, Sallam, and Elsayed, 2015), or things (Zhan, Wang, Cao, L. Li, and C. Li, 2010), provoking phenomena (A.K. Singha, H. Singha, Singhb, and Sawhneyb, 2002), change concentration of gases in the atmosphere (Gubb, Blanusa, Griffiths, and Pfrang, 2018).

As have been seen, quantification of relative humidity, which is derived from

environmental temperatures (Lin and Hubberd, 2003), is very important, due to its atmosphere-ocean interaction side effect, and also may be a useful parameter for forecasting (Ruano, Ferreira, and Mendes, 2010), hydro-climate studies (Lee, Zhan, and Pei, 2015), determine the consumption of energy in buildings (Mba, Meukam, Kemajou, 2016).

This project processed the relative humidity data from PMEL-NOAA (PMEL-NOAA) network to analyze particularities in time, a proposal that will be sustainable observing anomalies in the time series of each dataset, analyzing their trends, kind of oscillations (Yang, 2019), amplitudes. Discrete distribution functions to understand frequencies of occurrences and basic statistics. Finally, lag correlation functions, (Zebende, Brito, Silva, and Castro, 2018), between every pair of buoys of the grid to see trends between each couple. A small change in the lags of relative humidity (Rhee, Im, Kim, and Song, 2019) may be an important change in the atmosphere of the datasets (Ross et al, 2018), because of the repercussions in the adjacent areas (Sloane and Wolff, 1985), or any adjacent areas may influence in the ocean (Seidov et al., 2015). Relative humidity in this grid tends to be null in each dataset, discarding the options of covariance of any two datasets, and open another option, such parabolic relationship (El Massoud, 2005), or any chaotic system (McNeal, Petcovic, Bals-Elsholz, and Ellis, 2019).

## 2. MATERIALS AND METHODS

### 2.1. Data

This investigation pretended to examine the evolution in time of Relative Humidity in the Pacific Ocean, (Liua, Hana, Lia, Tianc, and Liud, 2018), trends (Bettio, 2008), normalized discrete distribution functions, and interprets interactions of Relative Humidity along the Equatorial Line in the Pacific Ocean. Reason why, annual data of relative humidity at 3 meters of altitude, between 137° E and 95° W meridians, and between 9° N and 8° S latitudes of sixty-nine buoys since 1980 (see figure 1), were handled from the Tropical Atmosphere Ocean / Triangle TransOcean Network (TAO/TRITO) project of the Pacific Marine Environment Laboratory (PMEL), directed by the National Oceanic and Atmospheric Administration (NOAA) around the equatorial line of the Pacific Ocean.

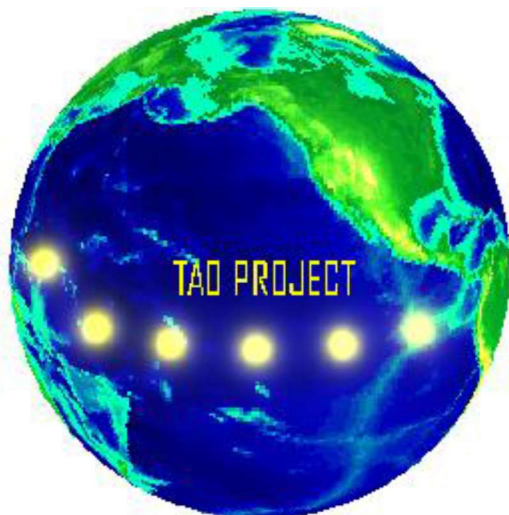


**Figure 1.** Location of the grid of Relative humidity located at the TAO/TRITON Project, in the Equatorial line of the Pacific Ocean of PMEL-NOAA. Adapted from MatLab (Mathworks Inc.).

## 2.2. Anomalies in Relative Humidity

The first arrangement was the analysis of sequential data, applied to time data collected from the whole moored instruments for the TAO/TRITON project, through their time series and their anomalies (Emery & Thomson, 2007), organized by latitudes and longitudes (Dare and Ebert, 2017). The trends and amplitudes vary along the time and may be an indicator in front of ENSO events, (Ambrosino, Thinová, Briestensky, and Sabbarese, 2019).

## 2.3. Statistical model

The second process applied to these data was the normalization of discrete relative distribution functions, (Cook, 2015) of the frequencies of occurrences of Relative Humidity, (Zhu L., Li, Y. & Jiang, Z., 2017). Considering a bin of one unit of size, for each dataset of the grid, "it will be represented a set of measured values,  $n_j$ , with  $j=1, \dots, m$ , in the finite widths elements (bins) of a partition of the range of allowed values of the dataset", (Pruneau, 2017) as indicated in Eq. 1, appreciating location, spread and symmetry of the pile of data, and the shapes of the probability density functions (Grace, 2015), and the number of humps (Wilks, 2006).

$$\text{frequency density} = \frac{\text{frequency}}{\text{class width}} \quad \text{Eq. 1}$$

Finally, the last arrangement was the analysis of trends of the temporal evolution of each buoy respect each other, dataset by dataset, it could be feasible to linearize them

respect each other by lag correlation functions, (Chung and Power, 2017, and Gerhards, Schramm, and Schmid, 2019), that avows figure out how well relative humidity of each dataset correlates in time respect to other datasets, defined in Eq. 2,

$$\tau(x, y) = \frac{\frac{1}{N-1} \sum_{i=1}^N (x_i - \bar{x})(y_i - \bar{y})}{\sqrt{\frac{1}{N-1} \sum_{i=1}^N (x_i - \bar{x})^2} \sqrt{\frac{1}{N-1} \sum_{i=1}^N (y_i - \bar{y})^2}} \quad \text{Eq 2}$$

where:

$\bar{x}$ : mean value of the  $x$  dataset ( $x$  buoy).

$\bar{y}$ : mean value of the  $y$  dataset ( $y$  buoy).

$N$ : length of the data set.

$x_i$ : any value of  $x$  dataset.

$y_i$ : any value of  $y$  dataset.

If  $\tau$  values trends to zero, means that relative humidity between the pair of buoys parameterized is scattered randomly without any relationship. The ranges could increase until  $\tau = 1$ , which means that datasets are dependent respect each other (Pickard and Emery, 2007).

All these processes were implemented using Matlab 2009a student version, and the codes were performed or adapted to this project from the functions of the software themselves.

## 3. RESULTS AND DISCUSSION:

### 3.1 Time evolution of relative humidity in the Pacific Ocean around the Equatorial line.

There should a relationship between temperature and moisture in the atmosphere of the tropical waters of the Pacific Ocean. It is known by the oceanographers that temperatures in this atmosphere have very small defined ranges as Relative Humidity does. In the Northeast of the Pacific Ocean, Relative Humidity fluctuates quasi harmonically inside the 64 % and 92 % interval of range around the continuous average line along the time. There would be appreciated an increment of Relative Humidity in some buoys in front of hot ENSO events (Wang and McPhaden, 2001), such in the 8° N 156° E and 8° N 165° E in 1997-98, as can be seen in figure 2, (a) and (b); and other lower peaks such 2000, as can be seen in figure 3, (a) and (b), in the 2° N 156° E buoy in the year 1998, and in the 2° N 165° E buoy in 1997, respectively.

Observing buoys located in the Southeast of the Pacific Ocean, the harmonic oscillations

have a major period of oscillations, achieving periods of 5 years around the continuous average value in the 0° N of latitude, see figure 4 (a), (0° N 156° E). But Southern latitudes have not standard behavior, presenting some of them, occurrences up the mean average value for more than 10 years, as can be seen in figure 4 (b). (5° S 156° E), and ranges of Relative Humidity are slightly bigger than northern buoys.

The time evolution of Relative Humidity in the Northwest of the Pacific Ocean almost oscillates harmonically with constant amplitudes around the average line, near the eastern surface. Abnormal oscillations are observed and, only in the 8° N 155° W, it is observed one wavelength up the time average line, 1997-98, and one oscillation below this line between 2013-14 in the 5° N 140° W buoys, see figure 5 (a) and (b), respectively.

In the Southwest of the Pacific Ocean, sinusoidal oscillations up and down the continuous average line are observed, but in the 8° S latitudes, as it is appreciated in the 5° S 170° W and 8° S 125° W positions, respectively, see figure 6 (a) and (b). Nevertheless, exceptions occur; some buoys do not oscillate during few years since 1997 as 5° S 155° W and 5° S 110° W buoys do. Past this period, there is another long period, almost 10 years, where occurrences happen above the time average line, it means, oscillations happen up this line, as indicates figure 6 (c) and (d).

There should an inverse or direct dependence of Relative Humidity with temperatures, depending on the location of the buoy, the reason why it will be recommended to correlate both variables. And also, it is seen that moisture is perturbed when an ENSO event is taking place.

### **3.2 Discrete Distribution Function of Relative humidity over the Pacific Ocean in the Equatorial line.**

It has been found a dependence on the occurrences of Relative Humidity respect colder or hotter periods in the Pacific Ocean around the Equatorial line. Besides, ranges are very similar in the east and the west sides of the grid. Observing annual histograms, it is seen that expected values for every buoy address to 80%, and extreme values do not exceed 60% in the lower limit and 94 % in the upper one. The shorter scale parameters of a probability density function of the observations are founded in the Northeast of the Pacific Ocean, see figure 7, (a) and (b); and the bigger ones in the Southwest

side, see figure 8, (a) and (b).

This contrast is reflected by the increase of means values of Relative Humidity in the west of the Pacific Ocean. The histograms at the 5° N latitude, just in the 155° W, 140° W, and 125° W meridians, have Gaussians shapes, but no one histogram has Gaussians shapes, see figure 9, (a), (b), and (c); major peaks are located in the eastern part of the Ocean, and lower peaks are located in the western part, achieving values of Relative Humidity of 100%, as could be seen in figure 10 (2° S 125° W).

By the seen in these histograms, it is possible to say that air temperature and relative humidity have a corresponding relationship in the area of the Pacific Ocean around the Equatorial line, and mean value increase in the west side of the network.

### **3.3 Linearization of Relative Humidity over the Pacific Ocean in the Equatorial line.**

Linearization of annual Relative Humidity in the Pacific Ocean over the Equatorial line between each pair of buoys shows that there are not a couple of buoys that correlate with each other. Observing plots of lag correlations of buoys located in the East of this area of the ocean, i.e. 0° N 156° E and 2° N 147° E, and 0° N 156° E and 2° N 165° E, see figure 11 (a), and (b), respectively; or buoys located in the west side, i.e. 0° N 125° W and 0° N 140° W, and 8° S 180° W and 9° N 140° W, see figure 12, (a) and (b), respectively; or buoys of the east and west of the Pacific Ocean, i.e. 0° N 156° E and 8° S 180° W, and 2° N 147° E and 8° S 180° W, see figure 13, (a) and (b), respectively, have around zero values along the time. It means that, every buoy has occurrences independently of each other; see figure 12, (a) and (b).

All the occurrences of lag correlation functions of relative humidity near the Equatorial line are very close to the expected values. In spite of that, it is appreciated that some buoys are perturbed several times, modifying slightly their directions. This fact is observed in the lag correlation between 0° N 156° E and 2° N 147° E, in the years 1997, 2004, 2001, as it could be seen figure 11 (a); in the lag correlation between 0° N 156° E and 2° N 165° E in 1997, 2002, 2006, and 2011, see figure 12 (b).

## **4. FUTURE PREDICTIONS:**

Analysis of relative humidity in front of temperatures, as SST, Air T, upper temperatures

(Wang and McPhaden, 2001) would be able to achieve an interaction forward ENSO events.

Taking short periods of time and subgrids (Weber and Mass, 2019) to linearize Relative Humidity, will allow focussing on variations of this parameter respect to ENSO events.

## 5. CONCLUSIONS:

It has been seen that some amplitudes of oscillations of time series of Relative Humidity are constants, and trend to oscillate periodically. Other buoys oscillate with variable amplitudes but with values near the extreme values of the ranges of Relative Humidity. Values of Relative Humidity for all the buoys oscillate harmonically; so, there should be a dependence of their expected value.

Occurrences of Relative Humidity oscillate in front of the time, but no one buoy synchronizes respect the others. These oscillations have small periods, especially in the Northern side of the Pacific Ocean, or large periods, especially in the Southern side of the ocean. Shapes of histograms are very similar, extreme values are characteristic of the side of the ocean, eastern or western, being bigger ranges near the American Continent. Even Relative Humidity of each buoy oscillates around 80%, no one buoy correlates with another buoy.

It is recommendable to compare short periods of time series of Relative Humidity in front of ENSO events since Relative Humidity is suitable for these events. And, also, a method to predict ENSO events means lag correlation functions, there would be working with shorter periods (Subramanian, Juricke, Dueben, and Palmer, 2019).

## 6. ACKNOWLEDGMENTS:

I would like to express my gratitude to Facultad de Ciencias and Facultad de Ingeniería Ambiental of Universidad Nacional de Ingeniería, Centro de Tecnologías de la Información y Comunicaciones (CTIC-UNI), and Clever for their cooperation on this Project. I would like to thank my Mother Teresa Chirinos, my Sister Teresa Díez, My wife Miriam Loayza and my two little children, Abbie and Paul, for enabling me to continue on this Project supporting and encouraging me in spite of all the time it took me away from them. I would like to greatly thanks Manuel and Raul Chirinos Coya for the orientation to develop the programs to process

the data for PMEL-NOAA.

## 7. REFERENCES:

1. Ambrosino, F., Thinová, Lenka., Briestensky, M., and Sabbarese, C. Anomalies identification of Earth's rotation rate time series (2012-2017) for possible correlation with strong earthquakes occurrences. *Geodesy and Geodynamics*, **2019**, 5.
2. Behar, O., Sbarbaro, D., Marzo, A., and Moran, L. A simplified methodology to estimate solar irradiance and atmospheric turbidity from ambient temperature and relative humidity. *Renewable and Sustainable Energy Reviews*, **2019**, 6.
3. Bettio, L. Seasonal climate summary southern hemisphere (winter 2007): a developing La Niña and a positive Indian Ocean Dipole. *Australian Meteorological Magazine*, **2008**, 11.
4. Buonocore, C., De Vecchi, R., Scalco, V., Lamberts, R. Influence of relative air humidity and movement on human thermal perception in classrooms in a hot and humid climate. *Building and Environment*, **2018**, 17.
5. Chakraborty, R., Talukdar, S., Saha, U., Jana, S., Maitra, A. Anomalies in relative humidity profile in the boundary layer during convective rain. *Atmospheric Research*, **2017**, 10.
6. Chung, Ch. T. Y. and Power, S. B. The nonlinear impact of El Niño, La Niña and the Southern oscillation on seasonal and regional Australian precipitation, **2017**, 21.
7. Cook, N. A statistical model of the seasonal-diurnal wind climate at Adelaide. *Australian Meteorological and Oceanography Journal*, **2015**, 23.
8. Cuxart, J and Jiménez, M. A. Mixing Processes in a Nocturnal Low-Level Jet: An LES Study. *Journal of the Atmospheric Science*, **2006**, 14.
9. Csavina, J., Field, J., Félix O., Corral-Avitia, A. Y., Sáez, A. E., Betterton, E. A. Effect of wind speed and relative humidity on atmospheric dust concentrations in semi-arid climates. *Science of the Total Environment*, **2014**, 8.

10. Dare, R. A., and Ebert, E. E. Latitudinal variations in the accuracy of model-generated forecasts of precipitation over Australia and South-east Asia. *Journal of Southern Hemisphere Earth System Science*, **2017**, 25.
11. El Massoud, M. On solvability of a parabolic system arising in physical oceanography. *Journal of Mathematical Analysis and Applications*, **2005**, 13.
12. Enrico Quagliarini, E., Gianangeli, A., D'Orazio, M., Gregorini, B., Osimani, A., Aquilanti, L., and Clementi, F. Effect of temperature and relative humidity on algae biofouling on different fired brick surfaces. *Construction and Building Materials*, **2019**, 9.
13. Emery, W. J., & Thomson, R. E. *Data Analysis Methods in Physical Oceanography*. Colorado, USA: Elsevier. **2006**.
14. Gehan, A.H., Sallam A, Elsayed, E.A. Estimating relations between temperature, relative humidity as independent variables and selected water quality parameters in Lake Manzala, Egypt. *Ain Shams Engineering Journal*, **2015**, 14.
15. Gerhards, C., Schramm, M., and Schmid, A. Use of the Weibull distribution function for describing cleaning kinetics of high-pressure water in the food industry. *Journal of Food Engineering*, **2019**, 26.
16. Gomez, B., Carter, L., Trustrum, N. A., Page, M. J., and Orpin, A. R. Coherent rainfall response to middle- and late-Holocene climate variability across the mid-latitude South Pacific. *The Holocene*, **2013**, 6.
17. Grace, W. Using the stretched Exponential Distribution to Model Runs of Extremes in a Daily Meteorological Variable. *Australian Meteorological and Oceanography Journal*, **2015**, 12.
18. Gubb, C., Blanusa, T., Griffiths, A., Pfrang, C. Can houseplants improve indoor air quality by removing CO<sub>2</sub> and increasing relative humidity? *Springer Nature*, **2018**, 11.
19. Ju, H. Y., Zhao, S. H., Mujumdar, A.S., Fang, X. M., Gao, Z. J., Zheng, Z. A., Xiao, H. W. Energy-efficient improvements in hot air drying by controlling relative humidity based on Weibull and Bi-Di. *Food and Bioproducts Processing*, **2018**, 44.
20. Klaassen, M., Schipper, D. J., Masen, M.A. Influence of the relative humidity and the temperature on the In-vivo friction behavior of human skin. *Biotribology*, **2016**, 31.
21. Kolehmainen, J., Sippola, P., Raitanen, O., Ozel, A., Boyce, Ch. M., Saarenrinne, P., and Sundaresan, S. Effect of humidity on triboelectric charging in a vertical vibrated granular bed: Experiments and modeling. *Chemical Engineering Science*, **2017**, 11.
22. Lawrence, M. G. The relationship between Relative Humidity and the Dewpoint Temperature in Moist Air. *Bulletin of the American Meteorological Society*, **2004**, 10.
23. Lee, H. F., Zhang, D. D., and Pei, Q. Reconstruction of the geographic extent of drought anomalies in northwestern China over the last 539 years and its teleconnection with the Pacific Ocean. *The Holocene*, **2015**, 14.
24. Liua, W., Hana, Y., Lia, J., Tianc, X., Liud, Y. Factors affecting relative humidity and its relationship with the long-term variation of fog-haze events in the Yangtze River Delta. *Atmospheric Environment*, **2018**, 8.
25. Lima, D. K., Ha Ahna, B., Jeongb, J. H. Method to control an air conditioner by directly measuring the relative humidity of indoor air to improve the comfort and energy efficiency. *Applied Energy*, **2018**, 9.
26. Lin, X. And Hubbard, K. G. Uncertainties of Derived Dewpoint Temperature and Relative Humidity. *American Meteorological Society*, **2003**, 4.
27. Maksic, J., Shimizu, M. H., Sampaio de Oliveira, G., Venancio, I. M., Cardoso, M., and Ferreira, F. A. Simulation of the Holocene climate over South America and Impacts on the vegetation. *The holocen*, **2018**, 13.
28. Mba, L., Meukam, P., Kemajou, A. Application of artificial neural network for predicting hourly indoor air temperature and relative humidity in modern building humid region. *Energy and Buildings*,

- 2016, 11.
29. McNeal, P., Petcovic, H., Bals-Elsholz, T., and Ellis, T. Seeing weather through chaos. *Bulletin of the American Meteorological Society*, **2019**, 14.
  30. Njau, E. C. Expressions for Wind Speed, Relative Humidity, Rainfall, Absolute Humidity, Vapor Pressure and Dew Point As Functions Of Temperature\*. *Renewable Energy*, **1994**, 6.
  31. Pickard, G. L., & Emery, W. J. *Descriptive Physical Oceanography. An Introduction*. Burlington, USA: Butterworth Heinemann, **2007**.
  32. PMEL-NOAA, N. O. *Global Marine Moored Buoy Array*. Retrieved from <https://www.pmel.noaa.gov/tao/drupal/disdel/>. **2015**.
  33. Pruneau, C. A. *Data Analysis Techniques for Physical Scientists*. New York: Cambridge University Press, **2017**.
  34. Rhee, J., Im, J., Kim, J., and Song, S. J. Humidity effects on the aerodynamic performance of a transonic compressor cascade. *International Journal of Heat and Mass transfer*, **2019**, 9.
  35. Riavo, N., Voarintsoa, G., Brook, G. A., Liang, F., Marais, E., Hardt, B., Cheng, H., Edwards R. L., and Railsback, L. B. Stalagmite multi-proxy evidence of wet and dry intervals in northeastern Namibia: Linkage to latitudinal shifts of the Inter-Tropical Convergence Zone and changing solar activity from AD 1400 to 1950. *The Holocene*, **2016**, 13.
  36. Ross, M. E., Vicedo-Cabrera, A. M., Kopp, R. E., Song, L., Goldfarb, D. S., Pulido, J., Warner, S., Furth, S. L., and Tasian, G. E. Assessment of the combination of temperature and relative humidity on kidney stone presentations. *Environment Research*, **2018**, 9.
  37. Ruano, A. E., Ferreira, P. M., and Mendes, H. MOGA Design of Temperature and Relative Humidity Models for Predictive Thermal Comfort. *IFAC Proceedings Volumes*, **2010**, 6.
  38. Sahin, S. & Cigizoglu, H. K. The effect of the relative humidity and the specific humidity on the determination of the climate regions in Turkey. *Springer / Verlag*, **2012**, 12.
  39. Seidov, D., Antonov, J. J., Arzayus, K. M., Baranova, O. K., Biddle, M., Boyer, T. P., Johnson, D. R., Mishonov, A. V., Paver, C., and Zweng, M. M. Oceanography north of 60° from World Ocean Database. *Progress in Oceanography*, **2015**, 21.
  40. Singha, A. K., Singha, H, Singhb, S.P., Sawhneyb, R.L. Numerical calculation of psychrometric properties on a calculator. *Building and Environment*, **2002**, 4.
  41. Sloane, Ch. S., and Wolff, G. T. Prediction of Ambient light scattering using a physical model responsive to relative humidity: Validation with measurements from Detroit. *Atmospheric Environment*, **1985**, 12.
  42. Subramanian, A., Juricke, S., Dueben, P., and Palmer, T. A stochastic representation of subgrid uncertainty for dynamical core development. *Bulletin of the American Meteorological Society*, **2019**, 11.
  43. Testaa, F., Maranob, G., Ambrogib, F., Boracchib, P., Casulac, A., Biganzolib, E., Moroni, P. Study of the association of atmospheric temperature and relative humidity with bulk tank milk somatic cell count in dairy herds using Generalized additive mixed models. *Research in Veterinary Science*, **2017**, 7.
  44. Uccellini, L. W., and Ten Hoeve, J. E. Evolving the National weather service to build a weather-ready nation. *Bulletin of the American Meteorological Society*, **2019**, 20.
  45. Weber, N. J. and Mass, C. F. Subseasonal weather prediction in a global convection-permitting model. *Bulletin of the American Meteorological Society*, **2019**, 11.
  46. Wang, W. and McPhaden, M. Surface Layer Temperature Balance in the Equatorial Pacific during the 1997-98 El Niño and 1998-99 La Niña. *Journal of Climate*, **2001**, 15.
  47. Wilks, D. S. *Statistical Methods in the Atmospheric Sciences*. USA. **2006**.
  48. Xiong Y., Meng Qing-Shi, Gao J., Tang Xiang-Fang, Zhang Hong-fu. Effects of relative humidity on animal health and welfare. *ScienceDirect*, **2017**, 6.
  49. Xu, J., Zhu, F., Wang, S., Zhao, X.,

- Zhang, M., Ge, X., Wang, J., Tian, W., Wang, L., Yang, L., Ding, L., Lu, X., Chen, X., Zheng, Y., Guo, Z. Impact of relative humidity on fine aerosol properties via environmental wind tunnel experiments. *Atmospheric Environment*, **2019**, 9.
50. Xu, X., Huang, Z., Zhang, X., and Li, Z. A novel humidity measuring method based on dry-bulb temperatures using artificial neural network. *Building and Environment*, **2018**, 8.
51. Yang, Z-Ch. Hourly ambient air humidity fluctuation evaluation and forecasting based on the least-squares Fourier-model. *Measurement*, **2019**, 12.
52. Zebende, A.A. Brito, A.M. Silva Filho, A.P. Castro. pDCCA applied between air temperature and relative humidity: An hour/hour view. *G.F. Physica A*, **2018**, 10.
53. Zhan, X., Wang, Y., Cao, L., Li, L., Li, Ch. Determining critical relative humidity by measuring air humidity in equilibrium directly. *European Journal of Pharmaceutical Sciences*, **2010**, 4.
54. Zhu L., Li, Y. & Jiang, Z. Statistical Modeling of CMIP5 Projected Changes in Extreme West Spells over China in the Late 21st Century. *Journal of Meteorological research*, **2017**, 18.

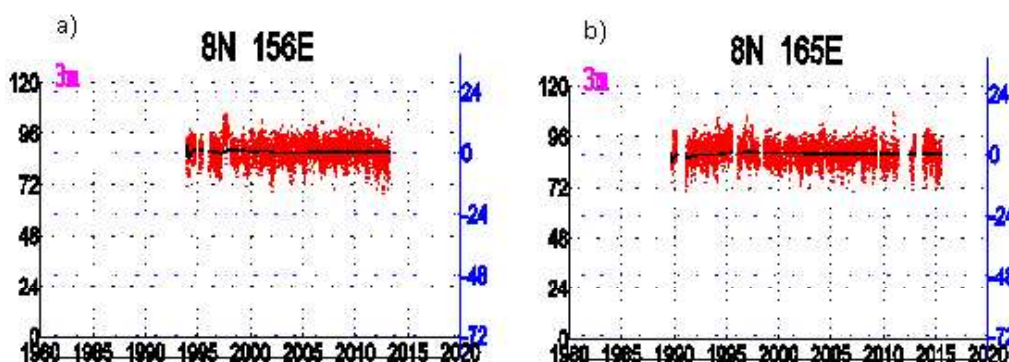


**Figure 2.** Increment of Relative Humidity occurrences above time average line at a) 8° N 156° E, b) and pronounced at 8° N 165° E.

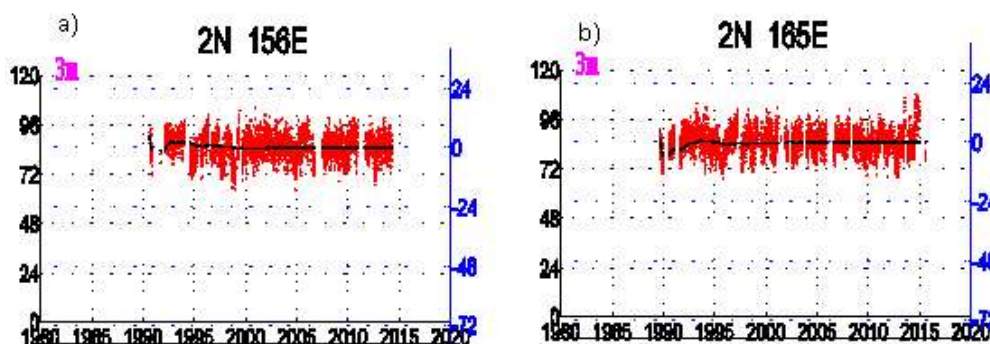


**Figure 3.** Reduction of Relative Humidity occurrences below time average line at a) 2° N 156° E, b) and pronounced at 2° N 165° E.



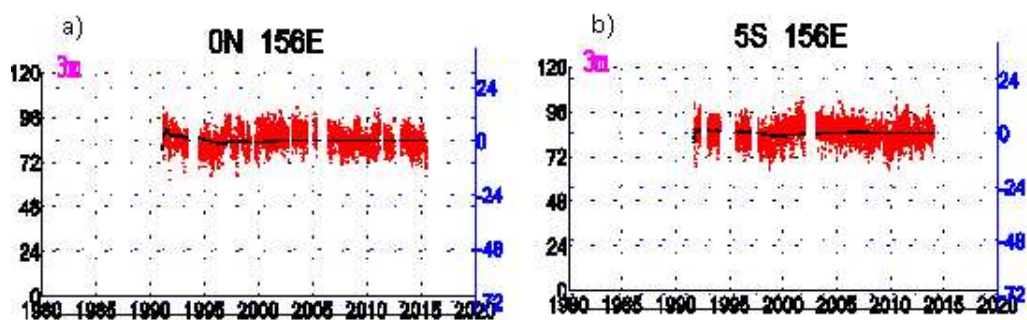


**Figure 4.** Normal oscillation of Relative Humidity above and below time average line during long period from 1997 at a)  $0^{\circ}$  N  $156^{\circ}$  E, and at b)  $5^{\circ}$  S  $156^{\circ}$  E.

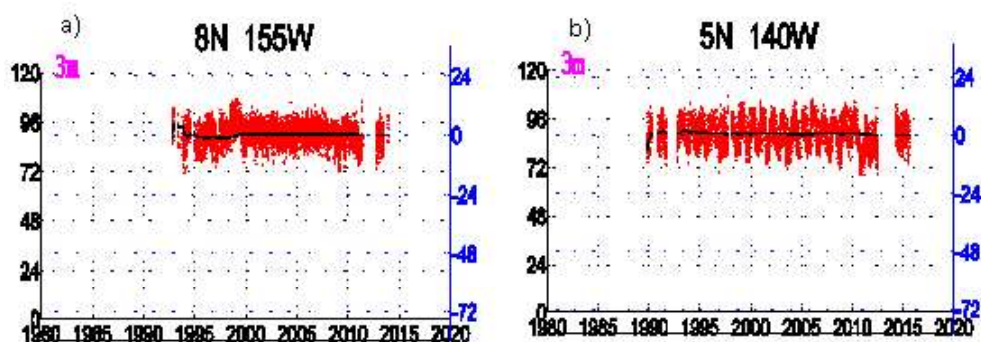


**Figure 5.** Abnormal oscillation of Relative Humidity in the northwest of the Pacific Ocean around the Equatorial line, oscillating a) above, at  $8^{\circ}$  N  $155^{\circ}$  W, and b) below, at  $5^{\circ}$  N  $140^{\circ}$  W, the time average line.

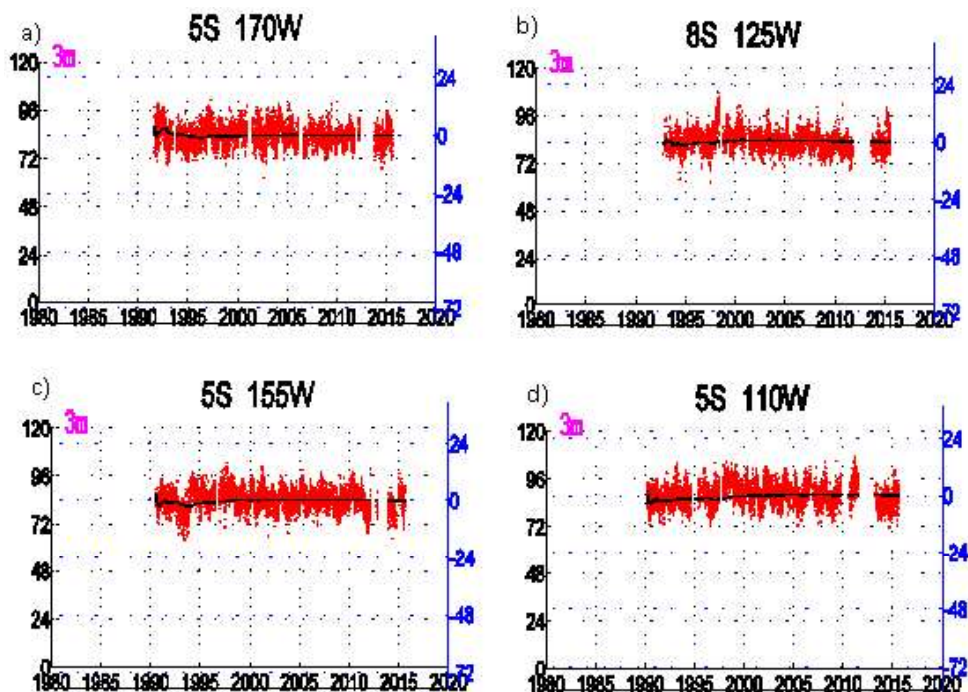


**Figure 6.** Sinusoidal oscillations of Relative Humidity in the southwest of the Pacific Ocean around the Equatorial line in normal conditions at a)  $5^{\circ}$  S  $170^{\circ}$  W, b)  $8^{\circ}$  S  $125^{\circ}$  W, and abnormal conditions at c)  $5^{\circ}$  S  $155^{\circ}$  W, and d)  $5^{\circ}$  S  $110^{\circ}$  W locations.

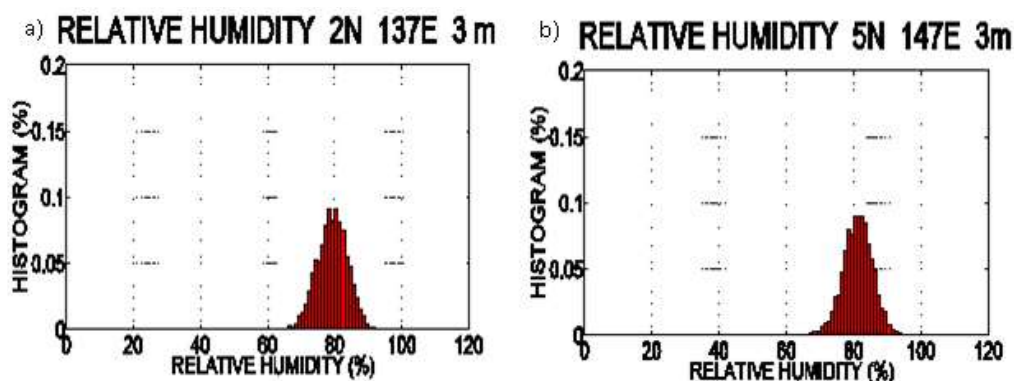


**Figure 7.** Discrete PDF of Relative Humidity in the northeast of the Pacific Ocean in the Equatorial line at a)  $2^{\circ}$  N  $137^{\circ}$  E, and b)  $5^{\circ}$  N  $147^{\circ}$  E.

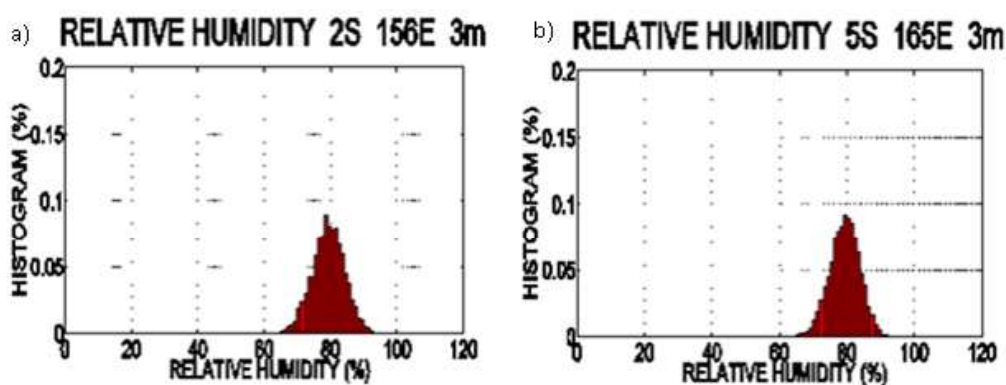


**Figure 8.** Discrete PDF of Relative Humidity in the southeast of the Pacific Ocean in the Equatorial line at a)  $2^{\circ}$  S  $156^{\circ}$  E, and b)  $5^{\circ}$  S  $165^{\circ}$  E.

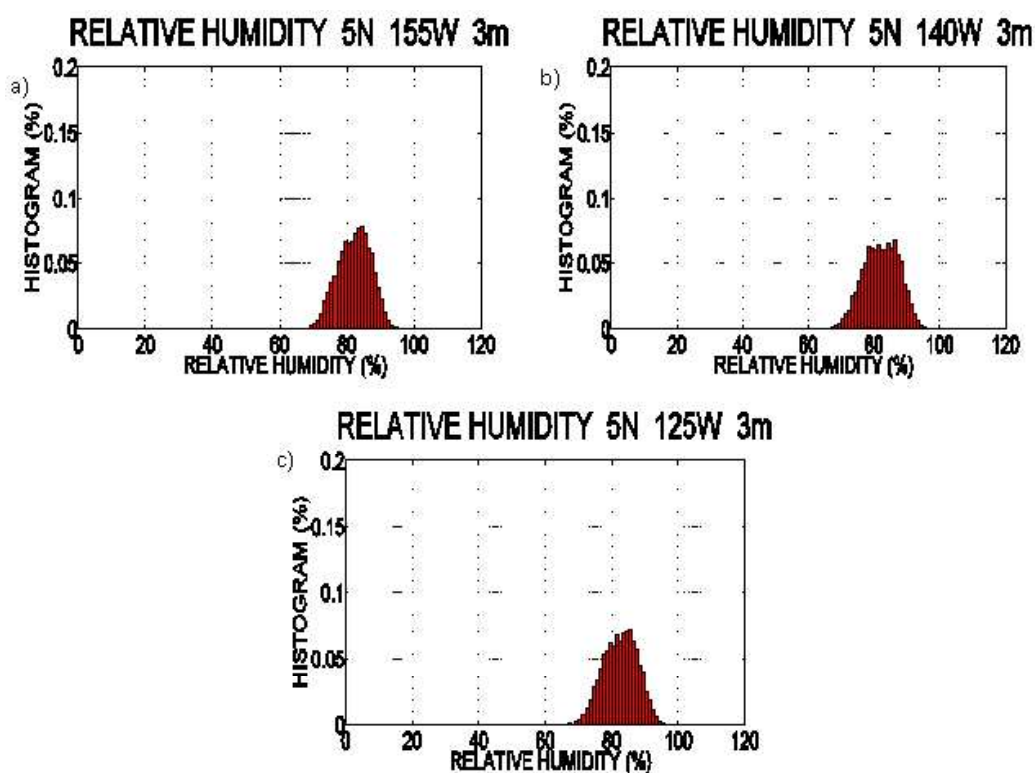


**Figure 9.** Gaussian shapes of Discrete PDF of Relative Humidity in the Pacific Ocean at the Equatorial line at a)  $5^{\circ}$  N  $155^{\circ}$  W, b)  $5^{\circ}$  N  $125^{\circ}$  W, and c)  $5^{\circ}$  N  $140^{\circ}$  W.

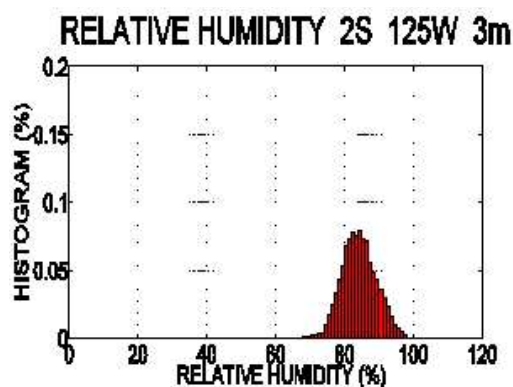


**Figure 10.** Lower peaks of Discrete PDF of Relative Humidity in the Pacific Ocean at the Equatorial line at 2° S 125° W.

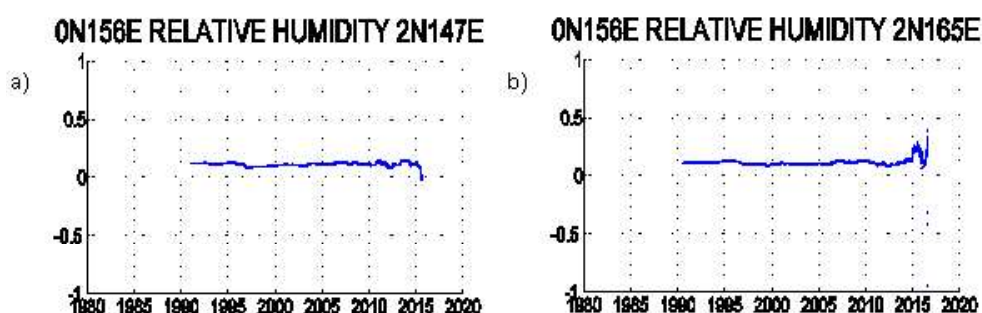


**Figure 11.** Lag correlation functions of PDF of Relative Humidity in the east side of the Pacific Ocean at the Equatorial line between a) 0° N 156° E and 2° N 147° E, and b) 0° N 156° E and 2° N 165° E.

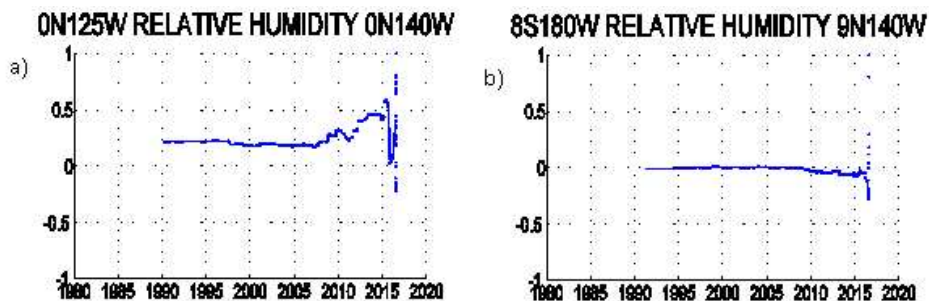


**Figure 12.** Lag correlation functions of PDF of Relative Humidity in the west side of the Pacific Ocean at the Equatorial line between a) 0° N 125° W and 0° N 140° W, and b) 8° S 180° W and 9° N 140° W.

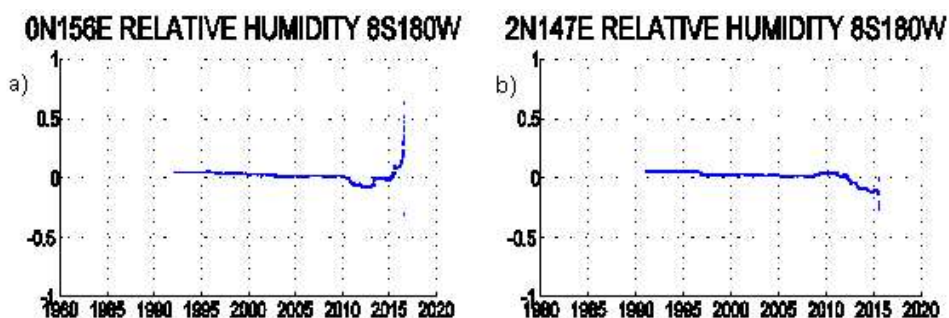


**Figure 13.** Lag correlation functions of PDF of Relative Humidity between the east and west sides of the Pacific Ocean at the Equatorial line between a) 0° N 156° E and 8° S 180° W, and b) 2° N 147° E and 8° S 180° W.